**Celal Bayar University Journal of Science**

# Assessment of Asphaltene Production on Fracture Aperture During Heavy Oil Recovery

Serhat Canbolat[1]*

[1] Petroleum and Natural Gas Engineering, Engineering Faculty, Near East University, Nicosia / TRNC, Mersin 10 – Turkey
*serhat.canbolat@neu.edu.tr
*Orcid: 0000-0002-7591-8276

Received: 9 January 2021
Accepted: 6 December 2021
DOI: 10.18466/cbayarfbe.857178

**Abstract**

During reservoir engineering analysis, the assessment of the possibility of asphaltene precipitation and corresponding heavy oil recovery with economic losses is carried out before any thermal operation. To investigate this phenomenon, three steam injection experiments using only steam, steam-$CO_2$, and steam-n-$C_4H_{10}$ at 1:1.29 volumetric ratios were carried out in naturally fractured limestone cores saturated with a 12.4° API heavy crude oil. After each experiment, the produced oil's asphaltene content was measured. Further, to determine the asphaltene effect on the fracture apertures and permeability, an improved cubic law (ICL) equation was used to determine the equivalent fracture aperture (EFA) change during the experiments. EFAs were calculated analytically. An initial observation made for only the steam injection experiment was a decline in asphaltene levels present in the producing oil. Asphaltene levels gradually increased as the effects of steam progressed. When $CO_2$ was added to the steam, the asphaltene content of the produced oil increased. Nevertheless, the asphaltene content increased in the produced oil did not change the fracture permeability and EFA considerably. In contrast, when n-$C_4H_{10}$ was injected with steam concurrently, the asphaltene levels gradually increased above the starting value. However, in the further injection period, the asphaltene content in the produced oil was lower than the starting value as the injection progressed. This indicated that a partial upgrading of the asphaltene in the rock matrix caused an improvement in the EFA.

**Keywords:** asphaltene content, EFA, hydrocarbon gas, ICL, steam injection, upgrading.

## 1. Introduction

Heavy crude oils contain significant quantities of asphaltene. Because these oils are extremely viscous and nearly immobile, it is critical to have a reservoir recovery mechanism in place to reduce the viscosity of the oil and allow it to flow into the well for production. Cyclic steam and steam-assisted gravity drainage (SAGD) types of thermal processes are based on viscosity reduction. The cyclic steam also includes an oil thermal expansion drive for growth. Alternatively, SAGD is mainly a gravity-based method of draining oil into horizontal production wells [1]. In this process, using the horizontal injector, a steam chamber is produced and the steam continuously flows around the chamber where the surrounding oil is condensed and heated. Heat is transferred by the latent heat of steam, conduction, and convection. Under the force of gravity, the heated oil drains to a horizontal production well situated at the reservoir's base. Steam can lead to changes in the behavior of the oil phase and the conditions of equilibrium that favor asphaltene deposition [1].

Asphaltene is generally described as crude oil fractions that are insoluble in n-heptane and soluble in benzene. Moreover, asphaltene is an amorphous form of hydrocarbon that is thought to be colloidally dispersed fine particles and partially soluble compounds found in crude oil [2]. Due to the size of the asphaltene, it is difficult to grasp the cycle of asphalt precipitation and agglomeration. Asphaltene can be dissolved in the oil reservoir and stored in crude oil as micelles or colloidal suspensions. When both resins and asphaltene are present, as in oil, on their incorporation, the asphaltene tends to associate preferentially with the resins [3].

When applying thermal EOR (enhanced oil recovery) methods to undersaturated reservoirs, the possibility of asphaltene precipitation and oil-wet inducement, among other potential issues, has become unavoidable and must be properly examined. In the case of saturated oil-wet reservoirs, on the other hand, wettability changes to water-wet can enable greater oil production than other mechanisms of thermal EOR methods [4].

The deposition of asphaltene from reservoir fluids is a serious problem during the production of oil as it may lead to plugging into the producer formation. In primary depletion of highly undersaturated reservoirs, either with hydrocarbon gas or injection of $CO_2$, asphaltene precipitation can occur [5].

The analysis of Batı Raman crude oil demonstrated an important and novel insight: increasing the concentration of saturates-fraction in the deasphalted oil resulted in greater asphaltene precipitation. This tendency is thought to be caused by impurities in crude oil's saturates fraction [6].

Ghahfarokhi et al. (2017) discovered that the two most significant factors influencing the rate of asphaltene deposition are flow rate and asphaltene concentration. The attachment of asphaltene particles to the surface reduces as the flow rate increases, resulting in more asphaltene particles in the solution. However, as more of an agent is applied, the concentration of asphaltene in the mixture rises, accelerating the deposition process [7].

While physical characterization studies revealed only moderate correlations between bulk sample density/viscosity and asphaltene content, it was discovered that the ratio of heavy fractions (resins + asphaltene) to light fractions (saturates + aromatics) has the greatest influence on crude oil viscosity and °API value. As this ratio increases, crude oil becomes more viscous and denser. The asphaltene/resin ratio was also found to be significant by zeta-potential tests due to its effect on asphaltene stability. The high asphaltene/resin ratios cause reduced asphaltene stability; however, this effect is compensated by the higher aromatics fraction in the bulk oil [8].

The effects of the asphaltene precipitation have been studied as part of a solvent-based recovery process such as Vapor Extraction (VAPEX). One of the advantages of asphaltene precipitation is the in-situ upgrading of the bitumen. This result suggests that asphaltene precipitation occurs when the injected solvent condenses and aggregates near the edge of the chamber, which potentially contributes to the in-situ upgrading of the bitumen [9].

To characterize the permeability damage caused by asphaltene deposition during a gas injection EOR process, a unique systematic technique was developed. Based on the fluid analysis conducted in this study, the tendency for asphaltene flocculation to occur under the expected operating conditions of gas injection in GOM Miocene reservoirs could be important. As the miscible front advances in the reservoir, the effect of decreased permeability is considered minor on the overall sweep performance [10].

All the aforementioned studies in the literature show that the precipitation of the asphaltene affects permeability, oil production, saturation, and thus, the equivalent fracture aperture of the reservoir. From this point of view, a new approach has gained importance for the analysis of the flow of heavy oil in the fractured medium during thermal methods. To investigate and analyze this phenomenon, an analytical approach has been used to evaluate the asphaltene production and precipitation when applying thermal EOR.

### 1.1 Assessment of Fracture Aperture

Typically, the cubic law (CL) has been improved and updated through testing on glass plates or concrete slabs rather than actual rock fractures. Nonetheless, some basic fluid flow problems in fractures, such as small-scale roughness, large-scale aperture variability, and high nonlinearity Reynolds number, have been established [11]. It assisted efforts to simulate the behavior of a single-phase flow in rough fractures. The flow tortuosity generated by fracture roughness has resulted in the development of pore-scale approaches such as channel models or the local cubic law (LCL), which better model local flow behavior by accounting for both aperture variance and, more recently, fracture layer ripple. The classical LCL, also known as the Reynolds equation, has been commonly implemented in fluid flow studies and convective and reactive solvent transport via a single fracture [12].

Early breakthroughs in the injection of water or aquifers can result in high-fluid transmission by fractures inside the reservoir. As a result, such analysis necessitates the understanding of the variation in the opening or aperture along the fracture [13]. Knowing the basics of fluid flow and the processes of transportation across related fractures is important. Comprehensive analysis of flow and transport processes inside complex networks of fractures continues to be a problem, as evidenced by studies based on isolated single rough-walled fractures [14, 15].

A modified cubic law (MCL) was first proposed by introducing a friction factor to account for the fracture roughness and tortuosity. Exact analysis of the flow system through rough and tortuous fractures helps to understand the problems of transportation in broken media. This can then provide a method for estimating efficient transport parameters based on the geometrical properties of the fracture [16].

Celal Bayar University Journal of Science
Volume 17, Issue 4, 2021, p 337-345
Doi: 10.18466/cbayarfbe.857178


In 2019, Canbolat and Parlaktuna developed the improved cubic law equation (ICL) for analyzing a flow system as;

$$Q = C \frac{b^3}{12\mu}\left(\frac{\Delta p}{L}\right) \quad \textbf{(1.1)}$$

where $Q$, flow rate (ml/min), $C$, coefficient, $b$, the equivalent fracture aperture (mm), $\mu$, the viscosity of flowing fluids (cp), $\Delta p$, the pressure difference between the inlet and outlet of the core holder (psi), and $L$ is the length of the fracture, which is the length of the core plug (mm). For fractured core flow analysis, the C coefficient for the ICL equation was assumed to be 0.60 [13].

In reservoir engineering research, experimental and/or modeling studies are needed to determine when, where, and how much asphaltene will precipitate. Steam injection experiments using only steam, steam-$CO_2$, and steam-n-$C_4H_{10}$ at 1:1.29 volumetric ratios are carried out in naturally fractured limestone cores saturated with a 12.4° API Batı Raman heavy oil. Asphaltene content is measured in the extracted oil during the study. The effect of in-situ upgrading or flocculation of the heavy oil using the asphaltene content is investigated. Hence, analytical calculations using the ICL equation are used to determine the asphaltene effect on the equivalent fracture apertures and the fracture permeability.

## 2. Materials and Methods

### 2.1. Experimental Set-up

The experimental set-up has four main parts. These are; 1. Fluid Injection System, 2. Core Holder, 3. Fluid Production System, 4. Data Recording and Controlling System. A schematic view of the experimental set-up is illustrated in Figure 1.

#### 2.1.1. Fluid Injection System

The fluid injection system consisted of a steam generator, $CO_2$, and n-$C_4H_{10}$ bottles. The steam generator used in the experiments is an electric steam boiler type that is suitable for laboratories. The generator was used to continuously produce steam at 40 psi and 140–150 °C during the experiments. The amount of noncondensable gas added to the steam was controlled and adjusted by a flowmeter. It was connected to the injection line, which was wrapped with a line heater and covered with an insulator to minimize heat loss during steam injection. Steam injection experiments were carried out with the presence of $CO_2$ and n-$C_4H_{10}$ in the steam at a volumetric ratio of 1:1.29.

#### 2.1.2. Core Holder

A schematic drawing of the core holder and experimental set-up is given in Figure 1. The properties of the core plugs and Batı Raman oil are given in Table 1. The viscosity alteration of crude oil as a function of temperature is given in Figure 2 accordingly.

**Table 1.** Naturally fractured core plug and heavy oil properties.

| | |
|---|---|
| **Rock Type** | Limestone |
| **Density (gr\cc)** | 2.61 |
| ***Porosity (%)** | 34-37 |
| ***Permeability (darcy)** | 0.1516 - 0.2424 |
| **Length (cm)** | 20.5 |
| **Diameter (cm)** | 5.08 |
| **API gravity (°API)** | 12.4 |
| **Asphaltene Content (weight %)** | 30 ± 5 (approximately) |

* Measured experimentally.

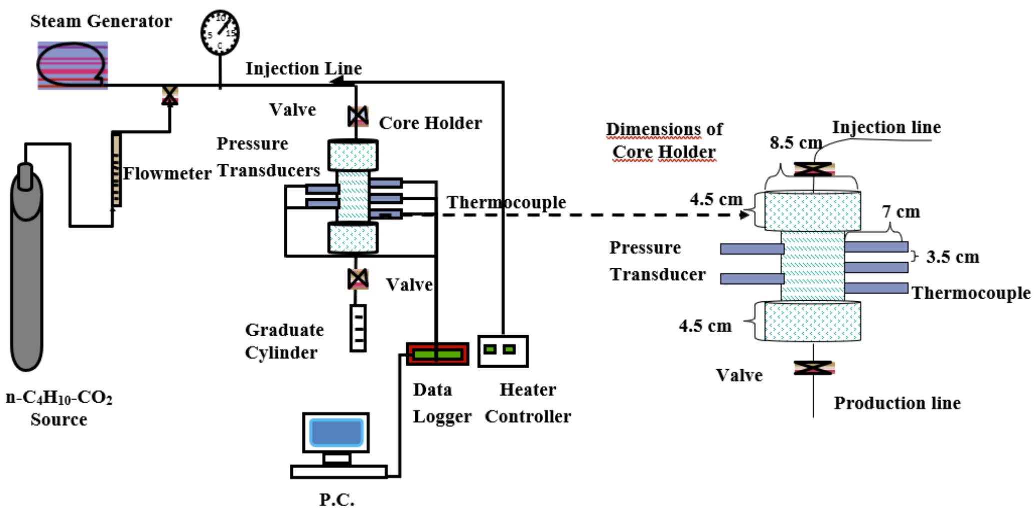


**Figure 1.** Experimental set-up & core holder.

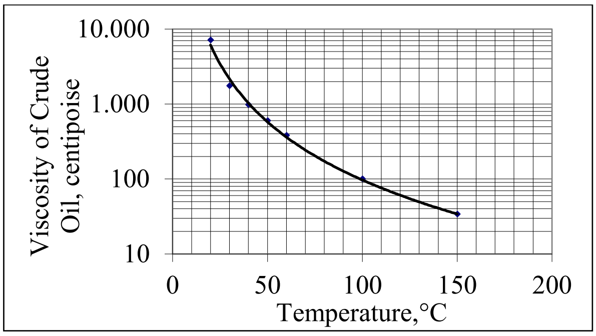


**Figure 2**. Viscosity alteration of the crude oil.

### 2.1.3. Fluid-Production System

During the experiments, the injection and production pressures were recorded at both ends using pressure gauges and pressure transducers. The input and output lines were covered with heaters and insulation material to reduce heat losses. The graduate cylinder collected the fluids produced and was placed below the core holder exit.

### 2.1.4. Data Recording and Controlling System

Data recording and the controlling system consist of thermocouples, a personal computer, and data loggers. Temperature distributions during the experiments were measured by 3 thermocouples connected to the core cell and then recorded in a data logger. The data records were continuously monitored by a personal computer using an excel spreadsheet.

## 2.2. Experimental Procedure

Before the experiments, the core plugs were completely saturated with the 12.4° API Batı Raman heavy oil. The core holder's temperature was raised to 50 °C. The heated and insulated injection line pumped superheated steam into the core holder at 40–55 psia and 140–150 °C. The production end of the core holder has been opened to the atmosphere. Both experiments were conducted until a preset steam-oil ratio and the recovery of oil were established. Besides, the temperature of the flow line and the temperature profile in the center were continuously measured and reported during each experiment. Following the experiments, core plugs were taken out of the core holder and put in the toluene extraction apparatus (SOXHLET) to determine saturation distribution after each experiment.

## 2.3. Asphaltene Measurements

The asphaltene measurement of the produced oil showed us the deposition, production, and sweep efficiency of the process applied to the system. Asphaltene measurements were carried out using toluene and hexane following the ASTM method. Toluene provided a dissolving effect for oil and hexane used for precipitation while measuring the asphaltene content of both produced oils [17].

Akmaz et al. (2011) reported the chemical analysis of Batı Raman crude oil and its asphaltene percent, respectively [6]. Batı Raman's heavy crude oil has high amounts of asphalt (28%), resin (27%), and aromatic fractions (26%). The amount of produced asphaltene in the oil was measured using samples taken from the produced fluids. The ratio of crude oil to hexane for the calculation of asphaltene content was taken at 1:10. One gram of oil was taken and mixed with 10 cc of hexane. Asphaltene particles were precipitated in the produced samples, and the weight percent of asphaltene was calculated in the oil. In this study, the measured asphaltene weight (Asp.W.) in Batı Raman heavy crude oil was 30%.

## 2.4. Porosity Measurement of Core Plugs

A mercury porosimeter was used to measure the porosity of the core plugs. The measured values of the porosity are given in Table 1.

## 2.5. Permeability Measurement of Core Plugs

The limestone core plugs' permeability ranges between 0.1516 and 0.2424 darcy, respectively. The permeability measurements of Core#1, 0.2424 darcy, Core#2, 0.1516 darcy, and Core#3, 0.2424 darcy were found respectively.

# 3. Results of the Steam Experiments

Oil wet limestone core plug experiments were performed. Three experiments were carried out in such a way that the system resembles a vertical cross-section of a reservoir of gravity drainage. The temperature of the process gradually increased for steam alone (Figure 3). For other systems, the ratio of the injected volume of steam was lower than the $CO_2$ and n-$C_4H_{10}$ injection volumes (1:1.29). Therefore, the temperature fluctuated around the temperature of the original core plug. (Figures 4, 5).

As a result, the steam could not be supplied at high temperatures and/or near high temperatures enough to reach the core plugs as it was generated in all experiments. It became hot water because of the decrease in permeability and the addition of $CO_2$ and n-$C_4H_{10}$ at room temperature. In the further production period, only in the steam case experiment, a steady temperature rise was observed. The steam-only oil recovery and steam-n-$C_4H_{10}$ cases are comparable (Figure 6). This may be due to the heterogeneity of the core plugs and fractures. However, the recovery of oil for adding $CO_2$ was lower than the other two. This may be due to the lower core plug permeability, although it took the longest time for the experiment. For both cases, the steam condensed at the core's entrance. In the steam-only case experiment, the early stages of steam chamber formation, described as the rising steam chamber, were seen [1].

Celal Bayar University Journal of Science
Volume 17, Issue 4, 2021, p 337-345
Doi: 10.18466/cbayarfbe.857178


**Table 2.** Improved cubic law analysis of the steam only experiment for equivalent fracture aperture and fracture permeability.

| Time | Pump Rate | Pressure Difference,ΔP | ICL Rate | Equivalent Fracture Aperture | Fracture Permeability, kf | Fracture Permeability, kf |
|---|---|---|---|---|---|---|
| hours | ml/min | bar | ml/min | mm | $cm^2$ | md |
| 0 | 0 | 0 | 0 | 0 | 0 | 0 |
| 00:58 | 0.370 | 0.180 | 0.370 | 0.235 | 2.17 E-09 | 217 |
| 01:58 | 0.370 | 0.180 | 0.370 | 0.235 | 2.17 E-09 | 217 |
| 02:43 | 0.370 | 0.200 | 0.370 | 0.227 | 1.95 E-09 | 195 |
| 03:22 | 0.370 | 0.220 | 0.370 | 0.219 | 1.77 E-09 | 177 |
| 03:55 | 0.370 | 0.200 | 0.370 | 0.227 | 1.95 E-09 | 195 |
| 04:24 | 0.370 | 0.180 | 0.370 | 0.235 | 2.17 E-09 | 217 |
| 04:49 | 0.370 | 0.160 | 0.370 | 0.244 | 2.44 E-09 | 244 |
| 05:15 | 0.370 | 0.220 | 0.370 | 0.219 | 1.77 E-09 | 177 |
| 05:36 | 0.370 | 0.210 | 0.370 | 0.223 | 1.85 E-09 | 185 |
| 05:57 | 0.370 | 0.200 | 0.370 | 0.227 | 1.95 E-09 | 195 |
| 06:14 | 0.370 | 0.180 | 0.370 | 0.235 | 2.17 E-09 | 217 |
| 06:34 | 0.370 | 0.160 | 0.370 | 0.244 | 2.44 E-09 | 244 |
| 06:50 | 0.370 | 0.200 | 0.370 | 0.227 | 1.95 E-09 | 195 |
| 07:05 | 0.370 | 0.192 | 0.370 | 0.230 | 2.03 E-09 | 203 |
| 07:18 | 0.370 | 0.192 | 0.370 | 0.230 | 2.03 E-09 | 203 |
| 07:28 | 0.370 | 0.180 | 0.370 | 0.235 | 2.17 E-09 | 217 |
| 07:34 | 0.370 | 0.160 | 0.370 | 0.244 | 2.44 E-09 | 244 |

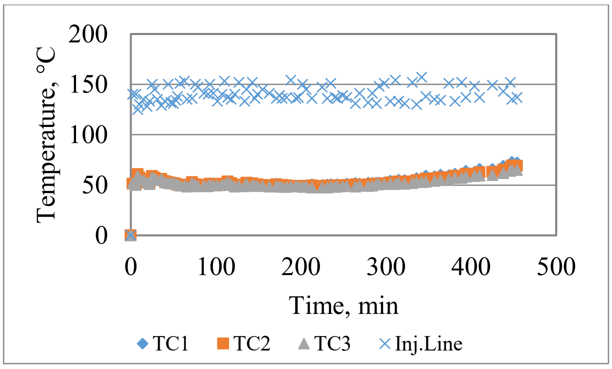


**Figure 3.** Temperature variation of core#2 during the steam-only experiment.

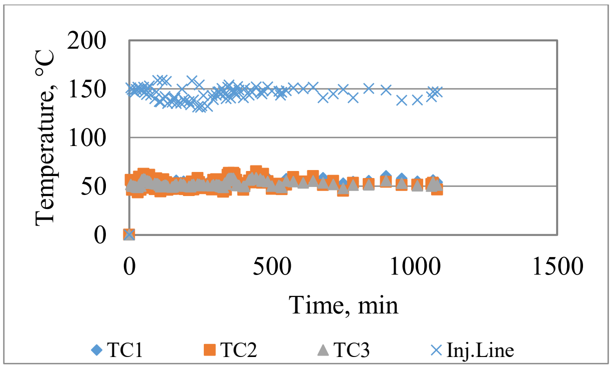


**Figure 5.** Temperature variation of core#4 during the steam+n-$C_4H_{10}$ experiment.

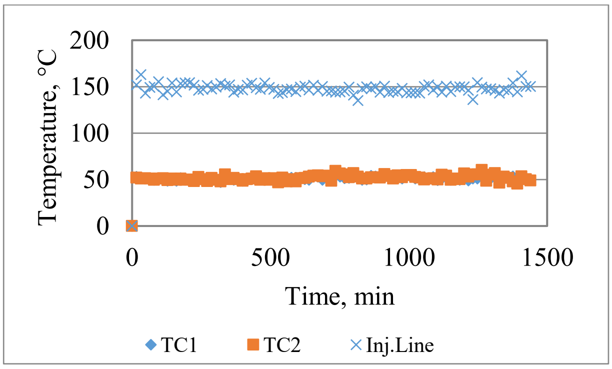


**Figure 4.** Temperature variation of core#3 during the steam+$CO_2$ experiment.

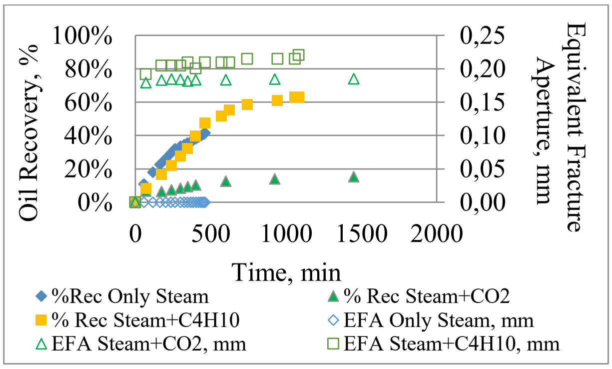


**Figure 6.** Effect of equivalent fracture aperture on % oil recovery.

Celal Bayar University Journal of Science
Volume 17, Issue 4, 2021, p 337-345
Doi: 10.18466/cbayarfbe.857178


Equivalent fracture aperture calculations showed that the variations due to flocculation affected the total recovery in the only steam case. However, $CO_2$ and n-$C_4H_{10}$ additions did not change the fracture aperture. However, the n-$C_4H_{10}$ addition case provided the highest recovery. Equivalent fracture aperture variations also changed the fracture permeability calculations of the core plugs. The steam-only case varied more with respect to $CO_2$ and n-$C_4H_{10}$ addition cases due to flocculation (Figures 7, 8) [13].

The influence of aperture on flow is often characterized by the steady-state solution to the Navier-Stokes equations for laminar viscous flow, which was improved as ICL and aforementioned in equation 1.1 [13]. Darcy's law and the ICL equation show that there is a direct relation between fracture permeability and equivalent fracture aperture. Higher EFA increased the fracture permeability (Figures 7, 8) [13].

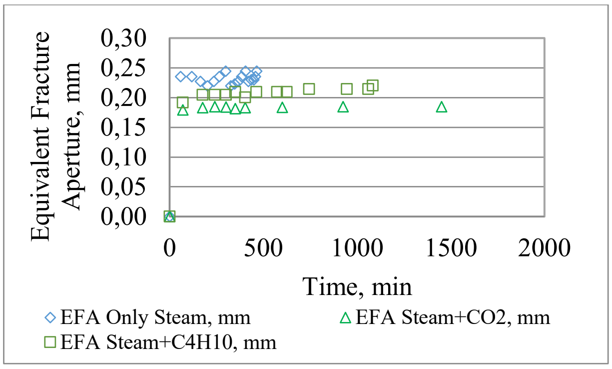


**Figure 7.** EFA variations.

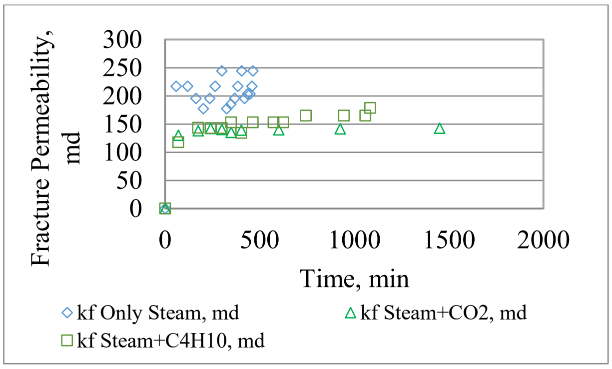


**Figure 8.** Fracture permeability variations.

To follow the variation during production, the initial asphaltene content of the heavy oil is shown with a dashed line on the graphs (Figures 9, 10). Measurements of asphaltene weight percent showed an increase in the asphaltene content of the oil originally produced in both cases (Figures 9, 10). Thus, partial upgrading was observed in core plug experiments. However, $CO_2$ addition to steam stabilized or decreased produced asphaltene content, showing adsorption of asphaltene at sites created by the injected steam with or without $CO_2$ gas. Nevertheless, the produced oil asphaltene content was decreased for the n-$C_4H_{10}$ addition below the initial value as the injection continued. This indicated partial upgrading of the asphaltene by the n-$C_4H_{10}$ addition [9].

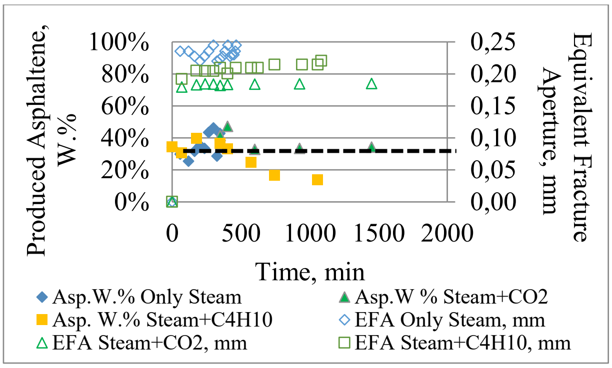


**Figure 9.** Effect of produced asphaltene on equivalent fracture aperture.

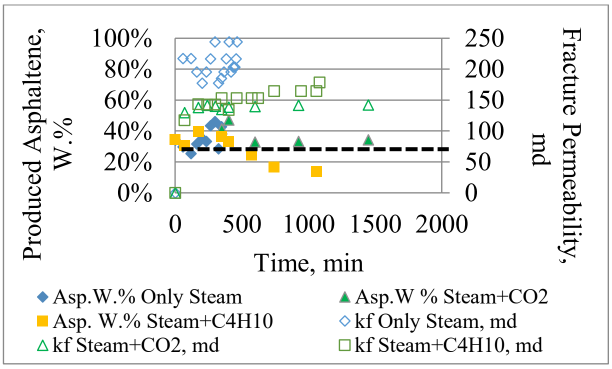


**Figure 10.** Effect of produced asphaltene on fracture permeability.

## 4. Discussions

Analytically, the equivalent fracture apertures were calculated for both core experiments using the ICL equation to observe the asphaltene effect on the equivalent fracture apertures and permeability. In the only steam injection case, an initial decrease in the asphaltene content of the extracted oil was observed (Table 2, Figure 9).

As the influence of steam progressed, the asphaltene content gradually increased. Therefore, the oil produced in situ was improved. Fracture permeability and equivalent fracture aperture were increased accordingly. The asphaltene content of the extracted oil indicates asphaltene remobilization (Figure 10) [9].

The addition of $CO_2$ to the steam increased the amount of produced oil with asphaltene content. The content of asphaltene has changed around the initial value (Table 3, Figure 9). The size of the non-uniform asphaltene deposition was comparable to that of the only steam case, but there was no significant impact on fracture permeability and equivalent fracture aperture due to the increased asphaltene content in developed oil (Figures 9, 10) [8].

In comparison, injecting n-$C_4H_{10}$ concurrently with steam raised the asphaltene content gradually above the initial value. Then the asphaltene content in the extracted oil was lowered below the initial value as the injection progressed in the further injection phase. This indicated a partial upgrading of the asphaltene in the rock matrix (Figures 9, 10). Moreover, n-$C_4H_{10}$ addition to steam also increased the equivalent fracture aperture and fracture permeability of the core, which verified the upgrading of oil (Table 4) [10].

**Table 3.** Improved cubic law analysis of the steam+$CO_2$ experiment for equivalent fracture aperture and fracture permeability.

| Time | Pump Rate | Pressure Difference,ΔP | ICL Rate | Equivalent Fracture Aperture | Fracture Permeability, kf | Fracture Permeability, kf |
|---|---|---|---|---|---|---|
| hours | ml/min | bar | ml/min | mm | cm$^2$ | md |
| 0 | 0 | 0 | 0 | 0 | 0 | 0 |
| 01:10 | 0.184 | 0.206 | 0.184 | 0.179 | 1.30 E-09 | 130 |
| 02:55 | 0.184 | 0.190 | 0.184 | 0.183 | 1.38 E-09 | 138 |
| 04:00 | 0.184 | 0.186 | 0.184 | 0.185 | 1.42 E-09 | 142 |
| 05:00 | 0.184 | 0.187 | 0.184 | 0.184 | 1.40 E-09 | 140 |
| 05:49 | 0.184 | 0. 194 | 0.184 | 0.182 | 1.35 E-09 | 135 |
| 06:42 | 0.184 | 0.183 | 0.184 | 0.183 | 1.39 E-09 | 139 |
| 10:00 | 0.184 | 0.188 | 0.184 | 0.184 | 1.40 E-09 | 140 |
| 15:25 | 0.184 | 0.185 | 0.184 | 0.185 | 1.42 E-09 | 142 |
| 18:25 | 0.184 | 0.185 | 0.184 | 0.185 | 1.42 E-09 | 142 |
| 21:10 | 0.184 | 0.183 | 0.184 | 0.186 | 1.43 E-09 | 143 |
| 23:55 | 0.184 | 0.182 | 0.184 | 0.186 | 1.44 E-09 | 144 |

**Table 4.** Improved cubic law analysis of the steam+n-$C_4H_{10}$ experiment for equivalent fracture aperture and fracture permeability.

| Time | Pump Rate | Pressure Difference,ΔP | ICL Rate | Equivalent Fracture Aperture | Fracture Permeability, kf | Fracture Permeability, kf |
|---|---|---|---|---|---|---|
| hours | ml/min | bar | ml/min | mm | cm2 | md |
| 0 | 0 | 0 | 0 | 0 | 0 | 0 |
| 01:10 | 0.203 | 0.183 | 0.203 | 0.192 | 1.17 E-09 | 117 |
| 02:55 | 0.203 | 0.185 | 0.203 | 0.203 | 1.43 E-09 | 143 |
| 04:00 | 0.203 | 0.186 | 0.203 | 0.205 | 1.43 E-09 | 143 |
| 05:00 | 0.203 | 0.188 | 0.203 | 0.205 | 1.43 E-09 | 143 |
| 05:49 | 0.203 | 0.181 | 0.203 | 0.209 | 1.53 E-09 | 153 |
| 06:42 | 0.203 | 0.197 | 0.203 | 0.200 | 1.34 E-09 | 134 |
| 07:43 | 0.203 | 0.183 | 0.203 | 0.209 | 1.53 E-09 | 153 |
| 09:34 | 0.203 | 0.179 | 0.203 | 0.209 | 1.53 E-09 | 153 |
| 10:24 | 0.203 | 0.177 | 0.203 | 0.209 | 1.53 E-09 | 153 |
| 12:22 | 0.203 | 0.170 | 0.203 | 0.214 | 1.65 E-09 | 165 |
| 15:45 | 0.203 | 0.167 | 0.203 | 0.215 | 1.65 E-09 | 165 |
| 17:39 | 0.203 | 0.170 | 0.203 | 0.215 | 1.65 E-09 | 165 |
| 18:04 | 0.203 | 0.160 | 0.203 | 0.220 | 1.78 E-09 | 178 |

### 4.1. Estimated Asphaltene Deposition after Steam Experiments

The asphaltene deposition of the experiments originated from the effective heating of the steam that was caused to produce all light fractions of the oil, sweeping through the core. This decreased the viscosity of the oil and increased the adsorption of asphaltene particles on limestone (Figures 9 and 10). % Recovery graphs of the only steam experiment have also supported this conclusion [4]. This can be explained by the fact that before reaching the injection line, the injected gas is at room temperature, so it takes a while to heat up. However, at the inlet of the core, the steam condenses, and the core temperature does not rise as non-condensing gas is added. The inlet temperature was still above the lower levels.

Celal Bayar University Journal of Science
Volume 17, Issue 4, 2021, p 337-345
Doi: 10.18466/cbayarfbe.857178 

Precipitation of asphaltene from reservoir fluids during oil withdrawal is a serious issue, as the deposition of asphaltene can cause the blockage of wells and production facilities. Asphaltene precipitation occurs for better oil recovery during primary depletion of highly unsaturated reservoirs that have a very low bubble point pressure or during hydrocarbon gas or $CO_2$ injection. This can also occur in heavy oil reservoirs during solvent injection. By changing the pH or solubility properties of the crude oil, asphaltene can be destabilized [18].

It was known that, from the analysis of Batı Raman crude, an increase in saturates-fraction concentration in the deasphalted oil resulted in more asphaltene precipitation. This trend is seen in the addition of n-$C_4H_{10}$ to steam, both by increased equivalent fracture aperture and fracture permeability of the core during the upgrading of oil [6].

The addition of n-$C_4H_{10}$ to steam also increased the destabilization of the asphaltene, making the residual oil more viscous and denser as the heavy fractions (resins + asphaltene) to light (saturates + aromatics) ratio increases. Since the heavier fractions were produced by the addition of n-$C_4H_{10}$ to steam, the residual water saturation increased [8].

Unbelievably, in the naturally fractured limestone core plug experiment, the steam-$CO_2$ case, due to the major chemical component of the core sample, which was $CaCO_3$, might have reacted with formed carbonic acid to cause the dissolution of calcite [19]. This might cause the dissolution of calcite after the interaction of $CO_2$-water-rock, which leads to the formation of a new texture in the core, plugging the pathway. That's why the recovery performance of the experiment cannot be realized as intended.

## 5. Conclusions

Precipitation and flocculation of asphaltene are considered problems of formation damage, which can reduce the recovery of oil. To analyze this phenomenon using a new approach, the asphaltene content of the produced oil was measured. The effect of asphaltene content on fracture apertures and permeability was investigated using the ICL equation. EFA change was calculated for the steam-only and $CO_2$/$C_4H_{10}$-addition cases.

1. For both core plug experiments, the EFAs were analytically calculated using the ICL equation to observe the asphaltene effect on the fracture aperture and permeability. Asphaltene levels slowly increased as the effects of steam progressed. Therefore, the produced oil was noted to improve in-situ. The fracture permeability and equivalent fracture aperture increased.

2. Comprising $CO_2$ in steam increased the asphaltene content of the produced oil. However, the asphaltene levels increased in produced oil did not change the fracture permeability and equivalent fracture aperture considerably.

3. On the contrary, when hydrocarbon gas n-$C_4H_{10}$ was introduced concurrently with steam, the levels of asphaltene increased slowly, and the content of asphaltene in produced oil decreased as the injection progressed, indicating a partial upgrade of asphaltene in the rock matrix.

4. The asphaltene deposition of the experiments originated from the effective heating of the steam that caused it to produce all the light fractions of the oil. Asphaltene flocculation was detected in only steam injection experiments by changing the equivalent fracture aperture and permeability.

## Future Work

This study provides an understanding of the asphaltene flocculation/alteration during steam with/without $CO_2$/n-$C_4H_{10}$ injection cases in an oil-wet reservoir. The equivalent fracture aperture variation was analyzed according to the precipitated and produced asphaltene. More investigation should be done to analyze the water-wet and mixed-wet reservoirs to see how the solvents and steam alter the asphaltene effect on the equivalent fracture aperture.

## Nomenclature

| | |
|---|---|
| A | : Cross-Sectional Area, $ft^2$ |
| b | : Fracture Aperture, mm |
| C | : Constant, (0.6) |
| CL | : Cubic Law |
| EFA | : Equivalent Fracture Aperture |
| ICL | : Improved Cubic Law |
| kf | : Fracture Permeability, md |
| L | : Length, cm |
| MCL | : Modified Cubic Law |
| Q | : Total Flow Rate, ml/min |
| $\Delta P$ | : Drawdown, psi |
| TC | : Thermocouple |

Symbols

| | |
|---|---|
| $\mu$ | : Fluid Viscosity, cP |
| $\phi$ | : Porosity, percent |

## Author's Contributions

Serhat CANBOLAT: Drafted and wrote the manuscript, performed the experiments, interpretations, and result in analysis with conclusions.

## Ethics

There are no ethical issues after the publication of this manuscript.

## References

**1.** Canbolat, S., Akin, S., and Kovscek, A. R., 2004, Non-condensable gas steam-assisted gravity drainage, *Journal of Petroleum Science and Engineering*, 45(1-2), 83-96.

**2.** Lee, K. S., Cho, J., Lee, J.H., 2020. $CO_2$ Storage Coupled with Enhanced Oil Recovery, ISBN 978-3-030-41901-1, 1st edn. Springer Nature eBook, Switzerland AG, 2020, pp 51-71.

**3.** Canbolat, S., Akin, S., Kovscek, A.R., 2006. Asphaltene Deposition During Steam-Assisted Gravity Drainage: Effect of Non-Condensable Gases, *Journal of Petroleum Science and Technology*; 24:1, 69-92.

**4.** Canbolat, S., Ozturk, H., Akin, S., 2021. Exploitation of Bati Raman field using advanced thermal methods: MAHOP VS. CSHP, *Journal of Petroleum Science and Engineering*; 208, (2022), 109802.

**5.** Oskui, G.P., Jurma, M.A., Abuhaimed, W.A., 2009. Laboratory Investigation of Asphaltene Precipitation Problems during $CO_2$/Hydrocarbon Injection Project for EOR Application in Kuwaiti Reservoirs, SPE 126267, SPE Kuwait International Petroleum Conference and Exhibition held in Kuwait City, 14-16 December.

**6.** Akmaz, S., Iscan, O., Gurkaynak, M. A., Yasar M., 2011. The Structural Characterization of Saturate, Aromatic, Resin, and Asphaltene Fractions of Batı Raman Crude Oil, *Petroleum Science, and Technology*; 29:2, 160-171.

**7.** Ghahfarokhi, A.K., Kor, P., Kharrat, R., Soulgani, B.S., 2017. Characterization of the asphaltene deposition process in flow loop apparatus; An experimental investigation and modeling approach, *Journal of Petroleum Science and Engineering*; 151, 330–340 January 2017.

**8.** Prakoso, A. A., Punase, A. D., Hascakir, B., 2017. A Mechanistic Understanding of Asphaltenes Precipitation From Varying-Saturate-Concentration Perspectives, *SPE Production & Operations*; pp 86-98, February 2017.

**9.** Kaito, Y., Kiriakehata, S., Nakagawa, K., Nakashima, H., Izumi, T., Yamada, T., 2020. Determination of Asphaltene Precipitation Amount under the Condition of the Solvent Assisted SAGD Process by the Application of PVT Apparatus SPE-199950-MS, e SPE Canada Heavy Oil Technical Conference originally scheduled to be held in Calgary, Alberta, Canada, 18 – 19 March.

**10.** Fassihi, M.R. Turek, E. and Honarpour, M.M., Fyfe, R., 2020. Investigation of Permeability Impairment Due to Asphaltene Precipitation During Gas Injection EOR in a Major GoM Field, SPE-200429-MS, SPE Improved Oil Recovery Conference held in Tulsa, OK, USA, 18 – 22 April.

**11.** Renshaw, C.E., Dadakis, J.S., Brown, S. R., 2000. Measuring Fracture Apertures: A Comparison of Methods. Geophysical Research. Letters, 27 (2), 289–292.

**12.** Brush, D.J., Thomson, N.R., 2003. Fluid Flow in Synthetic Rough- Walled Fractures: Navier-Stokes, Stokes and Local Cubic Law Simulations. *Water Resources Research*. 39 (4), 1085.

**13.** Canbolat, S., Parlaktuna, M., 2019. Analytical and Visual Assessment of Fluid Flow in Fractured Medium. *Journal of Petroleum Science and Engineering*; 173, 77–94 February 2019.

**14.** Zimmerman, R.W., Al-Yaarubi, A., Pain, C.C., Grattoni, C.A., 2004. Non-linear Regimes of Fluid Flow in Rock Fractures. *International Journal of Rock Mechanics and Mining Sciences*; 41 (1), 163–169.

**15.** Cardenas, M.B., Slottke, D.T., Ketcham, R.A., Sharp Jr., J.M., 2007. Navier-Stokes Flow and Transport Simulations Using Real Fractures Shows Heavy Tailing Due to Eddies. Geophysical Research. Letters; 34, L14404.

**16.** Wang, L., Cardenas, M.B., 2014. Non-Fickian Transport Through Two-Dimensional Rough Fractures, Assessment and Prediction. *Water Resources Research*; 50, 871–884.

**17.** Srivastava, R.K., Huang, S.S., Dong M., 1999. Asphaltene Deposition During $CO_2$ Flooding. *SPE Production & Facilities*; (November), 14 (4): 235-245.

**18.** Nghiem, L. X.,. Kohse, B. F., Farouq Ali, S.M., Doan, Q., 2000. Asphaltene Precipitation: Phase Behavior Modelling and Compositional Simulation, SPE-59432-MS, SPE Asia Pacific Conference on Integrated Modelling for Asset Management, Yokohama, Japan, 25-26 April.

**19.** Xiao, N., Li, S., Lin, M., 2017. An Investigation of $CO_2$-Water-Rock Interactions During $CO_2$ Flooding, *Electronic Journal of Geotechnical Engineering*; 2017 (22.05), pp 1629-1642.